
**Liquid Crystals**
Publication details, including instructions for authors and subscription information:
http://www.informaworld.com/smpp/title~content=t713926090

# Flexoelectric deformations of homeotropic nematic layers in the presence of ionic conductivity

Grzegorz Derfel[a]; Mariola Buczkowska[a]
[a] Institute of Physics, Technical University of Łódź, ul. Wólczańska 219, 93-005 Łódź, Poland

**To cite this Article** Derfel, Grzegorz and Buczkowska, Mariola(2005) 'Flexoelectric deformations of homeotropic nematic layers in the presence of ionic conductivity', Liquid Crystals, 32: 9, 1183 — 1190
**To link to this Article: DOI:** 10.1080/02678290500284405
**URL:** http://dx.doi.org/10.1080/02678290500284405

*Liquid Crystals*, Vol. 32, No. 9, September 2005, 1183–1190



# Flexoelectric deformations of homeotropic nematic layers in the presence of ionic conductivity

GRZEGORZ DERFEL* and MARIOLA BUCZKOWSKA
Institute of Physics, Technical University of Łódź, ul. Wólczańska 219, 93-005 Łódź, Poland

(*Received 14 January 2005; in final form 23 May 2005; accepted 8 June 2005*)

Elastic deformations of homeotropic nematic liquid crystal layers subjected to a d.c. electric field were studied numerically in order to find the dependence of threshold voltage on the properties of such a system. A nematic material characterized by a negative sum of flexoelectric coefficients and by a small negative dielectric anisotropy was considered. The flow of ionic current was taken into account. The electric properties are described in terms of a weak electrolyte model. Finite surface anchoring strength was assumed. The director orientation, the electric potential and the ion concentrations were calculated as functions of the coordinate normal to the layer. It was found that the threshold for the deformation depends on the distributions of the ions, governed by the generation constant and by the properties of the electrodes. The effects observed may be interpreted as a consequence of the separation of the ions. When the electrodes have pronounced blocking character, a high and non-uniform electric field, created by the subelectrode ion space charges, causes drastic decrease of the threshold voltage, much below the value $U_f$ valid for the insulating nematic. On the other hand, the electric field gradient arising in the bulk at moderate concentrations has a stabilizing effect and remarkably enhances the threshold above $U_f$. When the electrodes are conducting there are no significant space charges and the threshold voltage remains close to $U_f$. These results indicate that phenomena related to the charge transport should be taken into account in the analysis of the elastic deformations of ion-containing flexoelectric nematics.



## 1. Introduction

The interactions of a nematic liquid crystal with an external electric field are primarily due to the dielectric anisotropy of the liquid crystalline medium [1]. The applications of nematic liquid crystals in display devices are based on director field deformations induced by these interactions. Nevertheless several other effects contributing to these deformations are also considered: flexoelectricity [2], surface polarization [3] and ion adsorption [4, 5]. In particular, the ions, usually present in the liquid crystal material, have an important influence on the electric field distribution within the sample and therefore affect the field-induced deformations [6, 7].

In previous papers [8, 9], the threshold voltage for deformations of flexoelectric nematic containing ions was studied numerically under the assumption of perfectly blocking electrodes. It was shown that the threshold voltage decreased significantly providing that the flexoelectric properties were sufficiently strong, the surface anchoring was sufficiently weak and the ion concentration was sufficiently high. This decrease was attributed to the strong and highly inhomogeneous electric field which arose in the vicinity of the electrodes under these circumstances.

In the present paper, we move away from the idealized assumption of blocking electrodes. We perform numerical calculations in which the current flow across the layer is admitted. For this purpose, we have adopted a simplified model for electrical phenomena taking place at the nematic–electrode interface, as well as the weak electrolyte model for the bulk nematic [10]. The computations concerned the homeotropic layer of a weakly anchored nematic with negative dielectric anisotropy and negative sum of flexoelectric coefficients. Our main aim was to determine the effect of the electric current flow on the deformations of the nematic possessing flexoelectric properties.

The results show that the blocking character of the electrodes is the fourth condition necessary for the decrease of the threshold voltage. If this condition is not satisfied, the steady current flowing across the layer diminishes the ion concentration at the electrodes and therefore reduces its influence on the director field distortions. In brief, the threshold voltage for the deformation depends strongly on the average ion concentration when the electrodes have pronounced

*Corresponding author. Email: gderfel@p.lodz.pl

*Liquid Crystals*
ISSN 0267-8292 print/ISSN 1366-5855 online © 2005 Taylor & Francis
http://www.tandf.co.uk/journals
DOI: 10.1080/02678290500284405

blocking character, whereas it is practically constant when the electrode–nematic contacts are well conducting.

In the next section, the parameters of the system under consideration and the basic equations are given. In § 3, the results of calculations are presented; § 4 is devoted to their discussion.

## 2. Method

### 2.1. *Geometry and parameters*

The material and layer parameters were the same as in our previous paper [8]. A nematic liquid crystal layer of thickness $d=20\,\mu m$ was confined between two infinite plates parallel to the $xy$-plane of the Cartesian coordinate system. They were positioned at $z=\pm d/2$, and played the role of electrodes. The voltage $U$ was applied between them; the lower electrode ($z=-d/2$) was earthed. Homeotropic alignment was assumed. The anchoring strength $W$ was identical on both surfaces and was equal to $2\times10^{-5}\,J\,m^{-2}$. The director **n** was parallel to the $xz$-plane; its orientation was described by the angle $\theta(z)$, measured between **n** and the $z$-axis. Most of the material parameters used in calculations were chosen according to the properties of the liquid crystal MBBA. The model substance was characterized by the elastic constants $k_{11}=6.2\times10^{-12}\,N$ and $k_{33}=8.6\times10^{-12}\,N$. Negative dielectric anisotropy was adopted with the dielectric constant components $\varepsilon_{\parallel}=4.7$ and $\varepsilon_{\perp}=5.4$. The flexoelectric properties were expressed by the sum of flexoelectric coefficients $e_{11}+e_{33}=-40\times10^{-12}\,C\,m^{-1}$ (the separate values of $e_{11}$ and $e_{33}$ are not essential in the geometry considered [2]).

The detailed nature of the ions responsible for the electrical conductivity of nematic liquid crystals is unclear. In general, the ions are treated as a consequence of impurities (e.g. [11–13]) but it is difficult to identify the kind of dissociating species or to determine exactly the parameters concerning their kinetics. Our calculations concern macroscopic phenomena, therefore knowledge of the detailed character of the ions is unnecessary. We use only concentrations of the ions, leaving aside the problem of their nature. Such an approach is commonly used in theoretical considerations (e.g. [7, 14, 15]).

The average ion concentration $N_{av}$ ranged from $10^{17}$ to $3\times10^{20}\,m^{-3}$. It was defined as

$$N_{av}=\frac{1}{2d}\left\{\int_{-d/2}^{d/2}[N^{+}(z)+N^{-}(z)]\,dz\right\} \qquad (1)$$

where $N^{\pm}(z)$ denote the concentrations of ions of corresponding sign.

The transport of the ions under the action of an electric field is characterized by their mobility and diffusion coefficients. It was assumed that the mobility of the positive ions was much smaller than that of the negative ions [16, 17]. The values used in calculations correspond to typical results of mobility measurements in various liquid crystals and reflect typical anisotropy of mobility: $\mu_{\parallel}^{-}=1.5\times10^{-9}$, $\mu_{\perp}^{-}=1\times10^{-9}$, $\mu_{\parallel}^{+}=1.5\times10^{-10}$, $\mu_{\perp}^{+}=1\times10^{-10}$ $m^2\,V^{-1}\,s^{-1}$, i.e. $\mu_{\parallel}^{\pm}/\mu_{\perp}^{\pm}=1.5$ [13, 18]. The Einstein relation was assumed for the diffusion constants: $D_{\parallel,\perp}^{\pm}=(k_B T/q)\mu_{\parallel,\perp}^{\pm}$ where $q$ denotes the absolute value of the ionic charge, $k_B$ is the Boltzmann constant and $T$ is the absolute temperature. The weak electrolyte model [10] was adopted in which the ion concentration was determined by the generation and recombination constants. The generation constant $\beta$ depends on the electric field strength $E$ according to the Onsager theory [15, 19]:

$$\beta=\beta_0\left(1+\frac{q^3}{8\pi\varepsilon_0\bar{\varepsilon}k_B{}^2T^2}E\right)$$

where $\bar{\varepsilon}=(2\varepsilon_{\perp}+\varepsilon_{\parallel})/3$. Its value corresponding to the absence of the field, $\beta_0$, was varied from $10^{18}$ to $10^{24}\,m^{-3}\,s^{-1}$ in order to control the ion concentration. The recombination constant $\alpha$ was equal to $4.5\times10^{-18}\,m^3\,s^{-1}$. It was calculated from the Langevin formula [15, 20]: $\alpha=2q\bar{\mu}/\varepsilon_0\bar{\varepsilon}$, where the average mobility is expressed by $\bar{\mu}=\left[\left(2\mu_{\perp}^{+}+\mu_{\parallel}^{+}\right)/3+\left(2\mu_{\perp}^{-}+\mu_{\parallel}^{-}\right)/3\right]/2$.

### 2.2. *Basic equations*

The aim of the computations is to find the stationary states of the layer in the presence of ionic current. Although in principle such a system is dissipative, the mechanical equilibrium is given by the same torque equation that describes the non-conducting case [21].

The problem is considered to be one-dimensional. The reduced co-ordinate, $\zeta=z/d$, is used in the following. The functions $\theta(\zeta)$ and $V(\zeta)$ which describe the director orientation and the potential distribution within the layer are determined by the torque equation:

$$\frac{1}{2}(k_b-1)\sin2\theta\left(\frac{d\theta}{d\zeta}\right)^2-\left(\sin^2\theta+k_b\cos^2\theta\right)\frac{d^2\theta}{d\zeta^2}+\frac{1}{2}\frac{\varepsilon_0\Delta\varepsilon}{k_{11}}\sin2\theta\left(\frac{dV}{d\zeta}\right)^2+\frac{1}{2}\frac{e_{11}+e_{33}}{k_{11}}\sin2\theta\left(\frac{d^2V}{d\zeta^2}\right)=0 \qquad (2)$$

and the electrostatic equation:

$$\rho(\zeta)d^2+\varepsilon_0\left(\varepsilon_\perp+\Delta\varepsilon\cos^2\theta\right)\frac{\mathrm{d}^2V}{\mathrm{d}\zeta^2}-\varepsilon_0\Delta\varepsilon\sin 2\theta\frac{\mathrm{d}V}{\mathrm{d}\zeta}\frac{\mathrm{d}\theta}{\mathrm{d}\zeta}$$
$$+(e_{11}+e_{33})\cos 2\theta\left(\frac{\mathrm{d}\theta}{\mathrm{d}\zeta}\right)^2+\frac{1}{2}(e_{11}+e_{33})\sin 2\theta\frac{\mathrm{d}^2\theta}{\mathrm{d}\zeta^2}=0 \tag{3}$$

where $k_b=k_{33}/k_{11}$ and $\rho(\zeta)=q[N^+(\zeta)-N^-(\zeta)]$ is the space charge density.

The transport of ions in the bulk is governed by two equations of continuity of the ion fluxes

$$d(\beta-\alpha N^+N^-)=\frac{\mathrm{d}J_z^\pm}{\mathrm{d}\zeta} \tag{4}$$

$$\text{where } J_z^\pm=\mp\frac{1}{d}\left(\mu_{zz}^\pm N^\pm\frac{\mathrm{d}V}{\mathrm{d}\zeta}-D_{zz}^\pm\frac{\mathrm{d}N^\pm}{\mathrm{d}\zeta}\right)$$

denotes the flux of ions of given sign, i.e. the numbers of ions which pass through a surface $\zeta=const$, counted per unit area and per unit time. The $z$-components of the mobility and diffusion coefficients are given by $\mu_{zz}^\pm=\mu_\perp^\pm+\Delta\mu^\pm\cos^2\theta$ and $D_{zz}^\pm=D_\perp^\pm+\Delta D^\pm\cos^2\theta$, respectively, where $\Delta\mu^\pm=\mu_\parallel^\pm-\mu_\perp^\pm$ and $\Delta D^\pm=D_\parallel^\pm-D_\perp^\pm$ denote the anisotropies of both quantities.

The boundary conditions for $\theta(\zeta)$ are determined by the equations

$$\pm\left\{\frac{1}{2}\frac{e_{11}+e_{33}}{k_{11}}\sin 2\theta(\pm 1/2)\frac{\mathrm{d}V}{\mathrm{d}\zeta}\bigg|_{\pm 1/2}-\left[\sin^2\theta(\pm 1/2)\right.\right.$$
$$\left.\left.+k_b\cos^2\theta(\pm 1/2)\right]\frac{\mathrm{d}\theta}{\mathrm{d}\zeta}\bigg|_{\pm 1/2}\right\}-\frac{1}{2}\gamma\sin 2\theta(\pm 1/2)=0 \tag{5}$$

for $\zeta=\pm 1/2$, where $\gamma=Wd/k_{11}$. The boundary conditions for the potential are $V(-1/2)=0$ and $V(1/2)=U$.

In order to establish the boundary conditions for the ion concentrations, a suitable description of the phenomena taking place at the electrode–nematic interface is necessary. For the purpose of the present numerical simulations, we propose a simple model, that allows us to perform calculations with as few parameters as possible. The corresponding equations should express the fact that the flux of ions of given sign that approach a chosen electrode (or move away from it) is equal to the net change in the number of ions resulting from the generation and neutralization processes at the electrode per unit area and per unit time. The speed of neutralization of the ions, $n_r^\pm$, is proportional to their concentration: $n_r^\pm=K_r^\pm N^\pm$, and the speed of generation, $n_g^\pm$, is proportional to the concentration $N_d$ of the neutral dissociable molecules: $n_g^\pm=K_g^\pm N_d$, where $K_r^\pm$ and $K_g^\pm$ are suitable constants of proportionality. In the case of zero applied voltage, the equilibrium state realizes in which $N^\pm=N_0=(\beta_0/\alpha)^{\frac{1}{2}}$. Therefore $K_r^\pm N_0=K_g^\pm N_d$. Since $N^\pm\ll N_d$, one may neglect the dependence of $N_d$ on $z$ and ignore the flux of the dissociable molecules. This enables us to determine $K_g^\pm$ if $K_r^\pm$ and $N_d$ are estimated. In general, $K_g^\pm$ and $K_r^\pm$ can be different for each electrode process. For simplicity however, we performed the calculations using a common value of $K_r$ for all neutralization processes as well as a common value of $K_g=K_rN_0/N_d$ for all generation processes at the electrodes.

The processes of charge transfer between the molecules or ions in the liquid crystal and the electrodes are limited by energy barriers arising between the liquid and electrodes. For example, the transfer of an electron from the cathode to a neutral molecule depends on the work function of the electrode as well as on the affinity of the electron to the molecule. Similarly, the transfer of an electron from a molecule to the anode depends on the ionisation energy of the molecule and also on the work function of the electrode. The rates of generation and neutralization of the ions at the electrodes can be interpreted in terms of a model in which they are determined by the activation energies $\varphi$ of corresponding electrochemical reactions. For example, the rate of neutralization of a negative ion occurring by the transfer of an electron from the ion to the electrode is equal to $K_r=k_r\exp(-\varphi/k_BT)$, where $k_r$ is a constant. (Absolute values of the parameters $\varphi$ and $k_r$ are not essential, only the resulting $K_r$ value is important.) A similar formula can be used for the generation constant of positive ions occurring by the transfer of an electron from a neutral molecule to the electrode. (In general, the energy barriers $\varphi$ can be of different height for every electrode process.) The energy barrier is affected by the electric field existing at the electrode, i.e. increased or decreased by $\Delta\varphi=EqL$, where $L$ is the thickness of the subelectrode region, of the order of several molecular lengths. In our calculations $L=10$ nm was assumed.

As a result of the above assumptions, the boundary conditions take the forms:

$$\mp\mu_{zz}^\pm N^\pm\frac{\mathrm{d}V}{\mathrm{d}\zeta}-D_{zz}^\pm\frac{\mathrm{d}N^\pm}{\mathrm{d}\zeta}=\left[-N^\pm K_r\exp(\pm\Delta\varphi/k_BT)\right.$$
$$\left.+N_0K_r\exp(\mp\Delta\varphi/k_BT)\right]d \text{ for } \zeta=-1/2 \tag{6}$$

$$\mp\mu_{zz}^\pm N^\pm\frac{\mathrm{d}V}{\mathrm{d}\zeta}-D_{zz}^\pm\frac{\mathrm{d}N^\pm}{\mathrm{d}\zeta}=\left[-N^\pm K_r\exp(\mp\Delta\varphi/k_BT)\right.$$
$$\left.+N_0K_r\exp(\pm\Delta\varphi/k_BT)\right]d \text{ for } \zeta=+1/2 \tag{7}$$

The left hand sides of these equations represent the fluxes of the ions at the electrodes. The first terms on the right hand sides denote the numbers of ions which are neutralized; the second terms denote the numbers of

ions generated at the electrodes in the course of accepting or donating electrons by neutral molecules. To our knowledge, the boundary conditions formulated in such a form have not been applied previously. However, the existence of the energy barriers as well as the activation character of the electrode processes have been considered [11, 22, 23]. The influence of the subelectrode electric field on the height of the barriers was taken into account in terms of the Schottky effect, which was proposed as a plausible mechanism of charge transport in liquid crystal layers.

In order to illustrate possible essentially distinct behaviours of the layer, the calculations were carried out with several different values of $K_r$: $10^{-7}$, $10^{-5}$, $3\times10^{-4}$, $5\times10^{-4}$ and $10^{-3}\,m\,s^{-1}$, whereas $N_d$ was taken as equal to $10^{24}\,m^{-3}$ in every case. The set of ten equations (2)–(7) was solved numerically. The director configurations-described by the angle $\theta(\zeta)$ — the electric potential distributions $V(\zeta)$, and the ion concentrations $N^{\pm}(\zeta)$ were calculated for various voltages and various generation constants $\beta_0$. The results allowed us to determine the threshold voltages $U_T$ for the deformations in the following way. The director distributions were calculated for several successively lowered voltages, including very small distortions, for which $\theta(\zeta)<1^\circ$. The angle $\theta_m=\theta(\zeta=0)$, which was chosen as a measure of the deformation, was plotted vs. the voltage. No rapid decay of $\theta_m$ was detected, which indicates that the transition between the distorted and undistorted structures is of second order. The plots $\theta_m(U)$ were extrapolated to $\theta_m=0$ which yielded the threshold voltage value with accuracy of 0.01 V. We find it sufficient for our purposes.



## 3. Results

The deformations of the initial homeotropic alignment are due to the torques which have twofold origin: dielectric and flexoelectric. They are expressed by the third and fourth term of equation (2) and by the first terms of equation (5).

### 3.1. *Threshold voltage*

All the deformations revealed by the calculated $\theta(\zeta)$ functions have threshold character. The threshold voltage depends on the generation constant $\beta_0$ as well as on the properties of the electrodes. These dependences are shown in figure 1, where the threshold voltage $U_T$ is plotted as a function of average ion concentration, $N_{av}$, for five values of $K_r$.

For $K_r=10^{-7}\,m\,s^{-1}$, when the electrodes have strong blocking properties, three ranges of $N_{av}$ can be distinguished. For very low average concentration

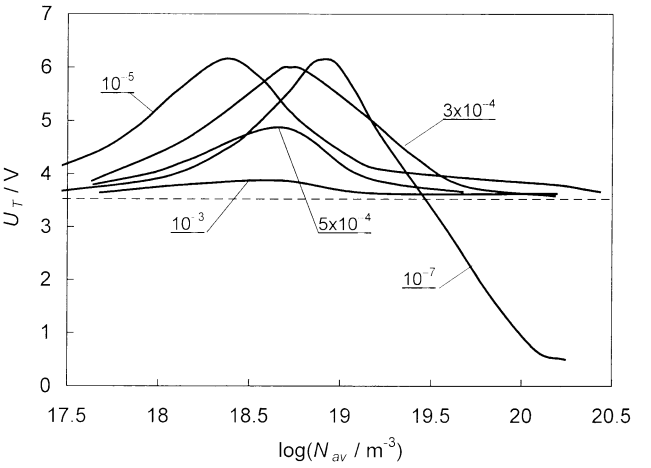


Figure 1. The threshold voltage $U_T$ as a function of average ion concentration $N_{av}$, for five values of $K_r$ indicated at each curve (in $m\,s^{-1}$). The dashed line represents the threshold $U_f=3.53$ V.

($10^{17}$–$10^{18}\,m^{-3}$), the threshold is close to the theoretical value $U_f=3.53$ V, calculated from the formula

$$\cot\left(\pi\frac{U_f}{U_c}\right)=\frac{Wd}{2\pi k_{33}}\frac{U_c}{U_f}\left\{\left(\frac{\pi k_{33}}{Wd}\frac{U_f}{U_c}\right)^2\left[\left(\frac{U_c(e_{11}+e_{33})}{\pi k_{33}}\right)^2+1\right]-1\right\} \qquad (8)$$

where $U_c=\pi(k_{33}/\varepsilon_0|\Delta\varepsilon|)^{\frac{1}{2}}$, [2]. It increases significantly with concentration up to 6.15 V at moderate $N_{av}$ value of c. $10^{19}\,m^{-3}$. At higher concentrations, the threshold decreases drastically to values as low as 0.5 V for $N_{av}\cong2\times10^{20}\,m^{-3}$.

For $K_r=10^{-5}\,m\,s^{-1}$, the ranges of low and moderate concentrations in which we observe similar behaviour as in the previous case are shifted towards lower values. The maximum threshold exceeding 6 V takes place at $N_{av}\cong2\times10^{18}\,m^{-3}$. Enhancement of $N_{av}$ does not reduce the threshold below $U_f$, and results in $U_T\cong3.7$ V instead of 0.5 V at $N_{av}\cong2\times10^{20}\,m^{-3}$. For $K_r=3\times10^{-4}\,m\,s^{-1}$, the $U_T(N_{av})$ dependence is similar but shifted to the higher concentrations. Further increase of $K_r$ reduces the maximum $U_T$ value which is illustrated by the curve plotted for $K_r=5\times10^{-4}\,m\,s^{-1}$. For $K_r=10^{-3}\,m\,s^{-1}$, i.e. for the well conducting electrodes, the threshold weakly depends on concentration. Its magnitude remains close to $U_f$ and varies between c. 3.6 and 3.8 V.

### 3.2. *Director distributions*

The deformations occurring at various average ion concentrations and starting from various threshold voltages have different character. A variety of director distributions is shown in figures 2 and 3 by means of

$\theta(\zeta)$ profiles plotted for voltages exceeding the threshold by 0.1 V.

Figure 2 shows the case for $K_r=10^{-7}\,m\,s^{-1}$. For low concentrations (curve 1), the deformation is very close to that predicted for a non-conducting nematic, which is described approximately by a combination of $\sin(\pi\zeta U/U_c)$ and $\cos(\pi\zeta U/U_c)$ [2]. At a somewhat higher concentration (curves 2 and 3) additional slight subsurface deformation of another type appears at $\zeta=-1/2$. At an even higher concentration, the deformation changes its character qualitatively, as illustrated by curves 4 and 5. Nevertheless, the singularity at $\zeta=-1/2$ does not disappear. The deformation becomes limited mainly to the region neighbouring the negative electrode. At last, when the ion concentration is high, another qualitative change occurs. The angle $\theta$ increases linearly with $\zeta$ except for narrow subelectrode regions, where rapid changes of orientation take place (curves 6 and 7). These profiles are very similar to those reported in [8] for blocking electrodes and are attributed to flexoelectric deformations resulting from a subsurface non-uniform field.

For $K_r=10^{-5}\,m\,s^{-1}$, similar behaviour takes place, but only for low and moderate concentrations (figure 3, curves 1– 4). The deformations are about twice as strong. For higher concentrations, the deformations have another character. The director deviation from initial homeotropic alignment is the largest in the middle of the layer (curves 6 and 7). There are also narrow regions adjacent to electrodes, where the director orientation changes rapidly.

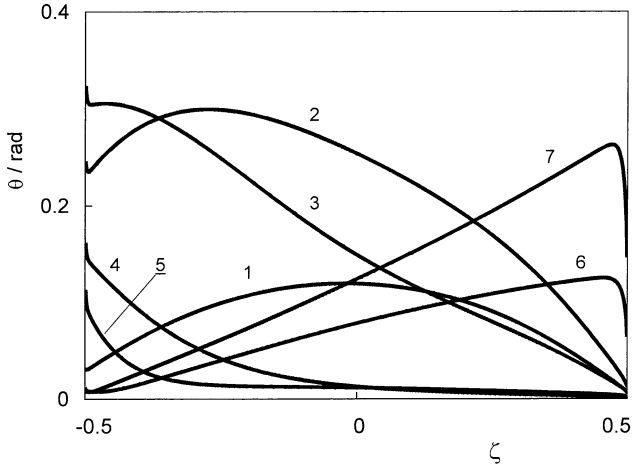


Figure 2. Director orientation angle $\theta$ as a function of the reduced coordinate $\zeta$ for $U=U_T+0.1$ V and $K_r=10^{-7}\,m\,s^{-1}$. Average ion concentrations (in $m^{-3}$) and voltages (in volts) are as follows. 1: $N_{av}=5.2\times10^{18}$, $U=5.64$; 2: $N_{av}=7.8\times10^{18}$, $U=6.25$; 3: $N_{av}=1\times10^{19}$, $U=6.12$; 4: $N_{av}=1.65\times10^{19}$, $U=4.86$; 5: $N_{av}=3.8\times10^{19}$, $U=3.15$; 6: $N_{av}=6.8\times10^{19}$, $U=1.85$; 7: $N_{av}=1.8\times10^{20}$, $U=0.60$.

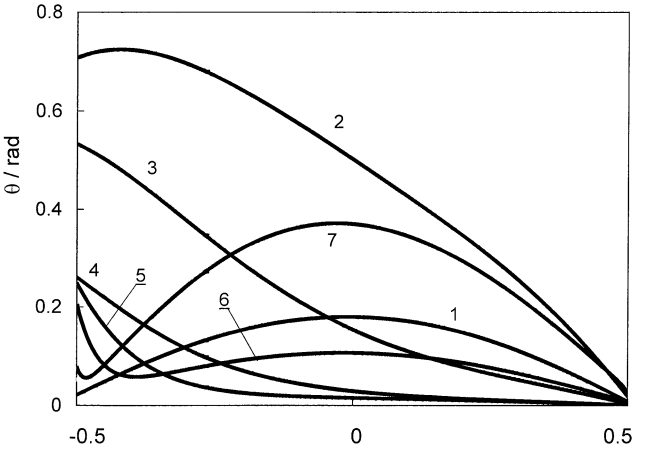


Figure 3. Director orientation angle $\theta$ as a function of the reduced coordinate $\zeta$ for $U=U_T+0.1$ V and $K_r=10^{-5}\,m\,s^{-1}$. Average ion concentrations (in $m^{-3}$) and voltages (in volts) are as follows. 1: $N_{av}=2.5\times10^{17}$, $U=4.17$; 2: $N_{av}=2.5\times10^{18}$, $U=6.26$; 3: $N_{av}=3.6\times10^{18}$, $U=5.90$; 4: $N_{av}=5.15\times10^{18}$, $U=5.32$; 5: $N_{av}=1.15\times10^{19}$, $U=4.42$; 6: $N_{av}=5.0\times10^{19}$, $U=4.03$; 7: $N_{av}=2.2\times10^{20}$, $U=3.85$.

The shape of the deformations of the highly conducting layer ($K_r=10^{-3}\,m\,s^{-1}$) is practically independent of the ion concentration. The corresponding profiles $\theta(\zeta)$ are nearly sinusoidal and very similar to those appearing at $K_r=10^{-7}$ and $=10^{-5}\,m\,s^{-1}$ for low concentration. Very slight departure from such a shape can be noticed for $K_r=5\times10^{-4}\,m\,s^{-1}$.

### 3.3. *Ion concentration and electric field strength*

The external voltage separates the ions and gathers them in the vicinity of the electrodes of opposite signs. The resulting space charge is particularly large when the electrodes are blocking and the average ion concentration is high due to high value of the generation constant $\beta_0$. Such a case is illustrated in figure 4 by curve pair 1 where the results for $K_r=10^{-7}\,m\,s^{-1}$ are presented. The bulk of the layer is electrically neutral. The concentrations at the surfaces are nearly two orders of magnitude higher than in the bulk. As a result, a high and non-uniform electric field arises in the vicinity of the electrodes, which is shown in figure 5 by curve 1. The subsurface sheets of the space charges significantly reduce the electric field in the bulk to about $0.1U/d$. At lower $N_{av}$, the ion concentrations are distributed inhomogeneously, which is due to greater mobility of the negative ions (figure 4, curve pairs 2 and 3). The layer becomes electrically charged as a whole, because the total number of positive ions is evidently larger than that of negative ions. The subsurface electric field becomes smaller. Its gradient also decreases and spreads over the prevailing part of the layer (figure 5, curve 2).

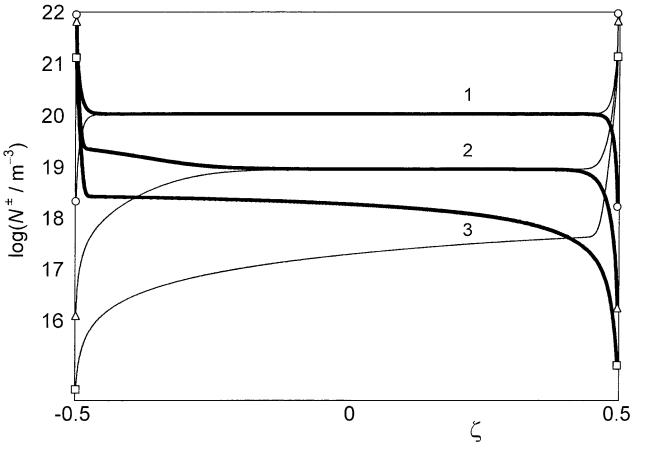


Figure 4. Ion concentrations as a functions of the reduced coordinate $\zeta$ for $K_r=10^{-7}\,m\,s^{-1}$; thick lines denote positive ions, thin lines denote negative ions. Average ion concentrations (in $m^{-3}$) and voltages (in volts) are as follows. 1: $N_{av}=1.8\times10^{20}$, $U=0.60$; 2: $N_{av}=3.8\times10^{19}$, $U=3.15$; 3: $N_{av}=7.8\times10^{18}$, $U=6.25$. Circles (1), triangles (2) and squares (3) permit identification of the concentration values at $\zeta=\pm1/2$.

At extremely low ion contents, the electric field strength is practically equal to $U/d$, with the exception of a very small excess field at the electrodes (figure 5, curve 3). Similar dependences were found for $K_r=10^{-5}\,m\,s^{-1}$, however at high ion concentrations the field strength in the bulk is not so radically reduced as previously and is very close to $U/d$.

For conducting electrodes, i.e. for $K_r=5\times10^{-4}$ and $=10^{-3}\,m\,s^{-1}$, the subsurface charges are so small that their influence on the electric field becomes unimportant. The inhomogeneous distribution of the ions gives rise to a gradient of the electric field in the bulk (figure 6).

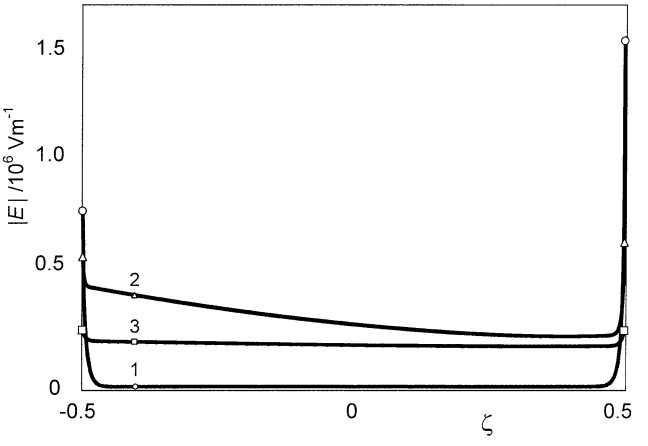


Figure 5. Electric field strength $|\mathbf{E}|$ as a function of the reduced coordinate $\zeta$ for $K_r=10^{-7}\,m\,s^{-1}$. Average ion concentrations (in $m^{-3}$) and voltages (in volts) are as follows. 1: $N_{av}=1.8\times10^{20}$, $U=0.60$; 2: $N_{av}=7.8\times10^{18}$, $U=6.25$; 3: $N_{av}=1.1\times10^{18}$, $U=4.06$. Circles (1), triangles (2) and squares (3) permit identification of the values of $|\mathbf{E}(\pm1/2)|$.

## 4. Discussion

In this paper, we consider the bias d.c. voltage-induced deformations of a nematic liquid crystal, a in which the flexoelectric properties play a crucial role. Deformations of this type are often referred to as the converse flexoelectric effect [24]. The main results of our calculations may be summarized as stated:

(a) Three ranges of the threshold voltage can be distinguished (figure 1): a threshold voltage close to the theoretical value $U_f$, if the ion concentration is low or if the average concentration is high and the electrodes are well conducting; a high threshold voltage at moderate ion concentrations; a very low threshold voltage at high concentrations and with blocking electrodes.
(b) Three types of director configuration occur above the threshold, depending on ion concentrations and electrode properties (figures 2 and 3).

These findings can be explained qualitatively by considering the electric field distributions which arise in the layer under various circumstances. First, the case of blocking electrodes ($K_r=10^{-7}\,m\,s^{-1}$) is analysed. The flexoelectric torque in the bulk of the layer is proportional to the electric field gradient $d\mathbf{E}/d\zeta$. In the case of high average ion concentration, this torque acts in the vicinity of the electrodes. In the vicinity of $\zeta=-1/2$,

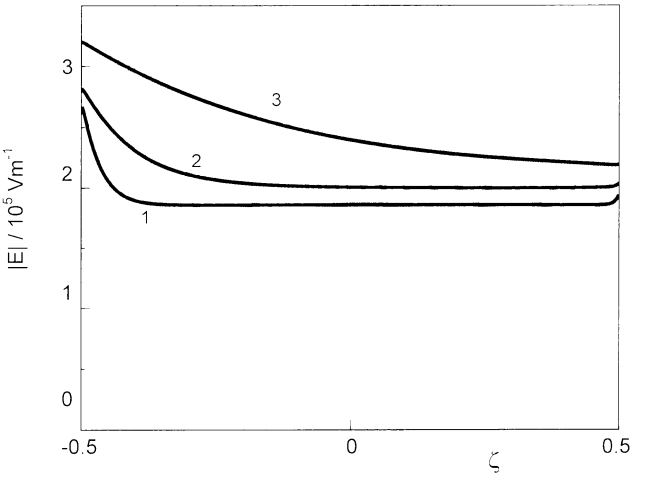


Figure 6. Electric field strength $|\mathbf{E}|$ as a function of the reduced coordinate $\zeta$ for $K_r=5\times10^{-4}\,m\,s^{-1}$. Average ion concentrations (in $m^{-3}$) and voltages (in volts) are as follows. 1: $N_{av}=4.8\times10^{19}$, $U=3.77$; 2: $N_{av}=1.5\times10^{19}$, $U=4.16$; 3: $N_{av}=4.7\times10^{18}$, $U=4.74$.

(where $d^2V/d\zeta^2 < 0$), it is opposite to the dielectric torque and therefore has a stabilizing effect. At $\zeta = 1/2$, (where $d^2V/d\zeta^2 > 0$), it co-operates with the dielectric torque, i.e. it gives rise to the deformation. The flexoelectric torque at the boundary surfaces is proportional to the electric field strength magnitude, $dV/d\zeta$. It has destabilizing effect at $\zeta = -1/2$ and quenches the deformation at $\zeta = 1/2$. Magnitudes of each of these four contributions depend on $N_{av}$.

At high ion concentrations, the $\mathbf{E}(\pm 1/2)$ values are extremely high and the electric field gradients are also very large. As a result, significant deformation in vicinity of $\zeta = 1/2$ is induced whereas any director deviation at $\zeta = -1/2$ is damped. In an analogous manner, some weak surface deformation occurs at $\zeta = -1/2$, but is damped in the vicinity of $\zeta = 1/2$. In the rest of the layer, the director distribution is adjusted to the subsurface orientation angles. The resulting deformations are illustrated in figure 2 by curves 6 and 7. They develop above the very low threshold voltage.

At moderate ion concentrations, the surface fields and subsurface field gradients are much smaller and do not exert sufficient torques. There is however the field gradient in the bulk; it induces a flexoelectric torque opposite to the destabilizing dielectric torque, which prevents deformation at low voltages. In consequence the threshold is enhanced to about 6.15 V.

At low ion concentrations, the flexoelectric torques both in the bulk and at the surfaces are negligible and the deformation typical for perfectly insulating nematic arises above the threshold which is close to $U_f$.

For $K_r = 10^{-5}\,m\,s^{-1}$, similar arguments can explain the threshold values observed at low and moderate ion concentration. For high concentrations however, the electric field at the surfaces and the subsurface field gradients are too small to induce deformations at low voltages and the threshold is close to $U_f$. For well conducting electrodes, $K_r = 10^{-3}\,m\,s^{-1}$, and the electric field is practically uniform and close to $U/d$. Therefore the threshold is close to the theoretical value $U_f$.

The qualitative explanation of the non-monotonic horizontal shift of the $U_T(N_{av})$ curves in figure 1 is difficult. The deformation arises if a subtle equilibrium between all the torques in the bulk (elastic, dielectric and flexoelectric) as well as at the boundary plates (elastic, flexoelectric and due to surface anchoring) is lost. All the torques are mutually related and connected with the ionic charge density. Numerical calculations seem to be the only way to predict the final effect of their competitive action. (We have found similar non-monotonic shifts for other cases of flexoelectric deformation.)

Keeping in mind the results of our previous papers [8, 9], one can mention four conditions for the appearance of the low threshold voltage: (i) high ion concentration, (ii) high flexoelectric coefficients, (iii) weak anchoring, and (iv) blocking electrodes.

One may expect that there are some similarities between the results obtained here for $K_r = 10^{-7}\,m\,s^{-1}$ and the results reported in [8], where perfectly blocking electrodes were assumed. Indeed, the profiles describing the deformations just above the low threshold, i.e. for high concentration, are qualitatively the same in the present paper (curves 6 and 7 in figure 2) and in [8]. On the other hand, important differences between the dependences of $U_T$ on ion contents are evident. In particular, the most distinguishing feature is the enhanced threshold which occurs at moderate ion concentrations due to the stabilizing field gradient in the bulk of the layer. This field gradient is determined by the asymmetric space charge distributions and by the difference in total numbers of positive and negative ions, and has its origin in the difference between $\mu^+$ and $\mu^-$ (and therefore between $D^+$ and $D^-$). In [8, 9] when the mobilities were not involved, the electric field distributions were practically symmetrical and there were no enhanced threshold voltages.

The importance of ion mobilities is confirmed by additional calculations performed for various relations between $\mu^+$ and $\mu^-$. Preliminary results show that for $\mu^+ = \mu^-$, the threshold at moderate concentrations is not enhanced and remains close to $U_f$. We will devote a separate paper to this study.

Other differences between the present results and the results obtained in [8] may be due to the processes of generation and recombination of ions, which are taken into account here but were ignored previously. These phenomena influence the ion distributions and therefore affect the electric field distributions.

In this paper, as well as in the previous one concerning the homeotropic layer [8], the negative sum of the flexoelectric coefficients was chosen. This choice determined the signs of the surface and bulk flexoelectric torques. The positive sum would give opposite torques. Preliminary computations show that in the case of $\mu^+ \neq \mu^-$ and $e_{11} + e_{33} > 0$, deformations have another shape and start at another threshold. The corresponding results will be presented in our next paper.

## References

[1] L.M. Blinov, V.G. Chigrinov. *Electro-optic Effects in Liquid Crystal Materials*. Springer Verlag, New York (1993).

[2] A. Derzhanski, A.G. Petrov, M.D. Mitov. *J. Phys. (Paris)*, **39**, 273 (1978).

[3] A.V. Zakharov, R.Y. Dong. *Phys. Rev. E*, **64**, 042701 (2001).
[4] G. Barbero, G. Durand. *Phys. Rev. A*, **35**, 1294 (1987).
[5] G. Barbero, L.R. Evangelista, N.V. Madhusudana. *Eur. Phys. J. B*, **1**, 327 (1998).
[6] G. Barbero, L.R. Evangelista. *Phys. Rev. E*, **68**, 023701 (2003).
[7] S. Ponti, P. Ziherl, C. Ferrero, S. Žumer. *Liq. Cryst.*, **26**, 1171 (1999).
[8] M. Felczak, G. Derfel. *Liq. Cryst.*, **30**, 739 (2003).
[9] M. Felczak, G. Derfel. *Proc. SPIE*, **5565**, 191 (2004).
[10] G. Briere, F. Gaspard, R. Herino. *J. chim. Phys.*, **68**, 845 (1971).
[11] S. Murakami, H. Naito. *Jpn. J. appl. Phys.*, **36**, 773 (1997).
[12] M.R. Costa, R.A.C. Altafim, A.P. Mammana. *Liq. Cryst.*, **28**, 1779 (2001).
[13] S. Naemura, Y. Nakazono, K. Nishikawa, A. Sawada, P. Kirsch, M. Bremer, K. Tarumi. *Mat. Res. Soc. Symp., Proc.*, **508**, 235 (1998).
[14] G. Barbero, D. Olivero. *Phys. Rev. E*, **65**, 031701 (2002).
[15] H. DE Vleeschouwer, A. Verschueren, F. Bougriona, R. van Asselt, E. Alexander, S. Vermael, K. Neyts, H. Pauwels. *Jpn. J. appl. Phys.*, **40**, 3272 (2001).
[16] H. Naito, M. Okuda, A. Sugimura. *Phys. Rev. A*, **44**, R3434 (1991).
[17] M.Y. Jin, J.-J. Kim. *J. Phys. condens. Matter*, **13**, 4435 (2001).
[18] G. Derfel, A. Lipiński. *Mol. Cryst. liq. Cryst.*, **55**, 89 (1979).
[19] L. Onsager. *J. chem. Phys.*, **2**, 599 (1934).
[20] P. Langevin. *Ann. Chem. Phys. (Paris)*, 7e serie, **28**, 433 (1903).
[21] I. Dozov, G. Barbero, J.F. Palierne, G. Durand. *Europhys. Lett.*, **1**, 563 (1986).
[22] A.V. Koval'chuk. *J. Phys.: condens. Matter.*, **13**, 10333 (2001).
[23] S. Naemura, A. Sawada. *Mol. Cryst liq. Cryst.*, **346**, 155 (2000).
[24] A.G. Petrov. In *Physical Properties of Liquid Crystals: Nematics*, D.A. Dunmur, A. Fukuda, G.R. Luckhurst (Eds), pp. 251–264, INSPEC, London (2001).